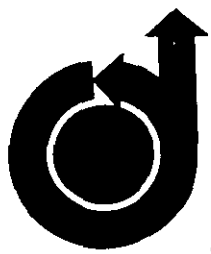

AIAA-80-1011

Noise from a Vibrating Propeller

H. L. Runyan, George
Washington University, NASA
Langley Research Center,
Hampton, Va.

AIAA 6th AEROACOUSTICS CONFERENCE

June 4-6, 1980/Hartford, Connecticut

NOISE FROM A VIBRATING PROPELLER

H. L. Runyan*
Joint Institute for Advancement of Flight Sciences
The George Washington University
Hampton, VA 23665

Abstract

This paper is concerned with an analytical study of the noise from a vibrating propeller. The influence of airfoil thickness as well as steady loading are also included in order to provide a basis for comparison. The analysis was based on the concept of distributing sources and doublets on the surface of the blade, which were multiplied by their appropriate strength factors. The noise in the plane of the propeller was dominated by the thickness noise. When the observation point was rotated 45° ahead of the propeller plane, the steady state load noise and the vibration noise were greater than the thickness noise. Moving the observer's position to the propeller axis, the thickness noise and loading noise were zero, and a pure sinusoidal noise was found, caused by the vibrations of the propeller.

Introduction

During acoustical testing of several propeller blades, some of the propellers exhibited a very sharp increase in noise at certain high rotational speeds. Examination of the data indicated the possibility that the blades might be experiencing propeller flutter. The exact rotational speed at which this occurred was not known. However, some simplified flutter calculations were made and indicated that the propellers could have fluttered in the test speed range.

A search of the literature indicated no theoretical research had been done in the area of noise produced by oscillating propeller blades. It is the purpose of this report to present the results of an analytical study of the problem. The basis of the method was developed in reference 1, in which a study was made aimed at determining the unsteady aerodynamic forces on an oscillating blade utilizing lifting surface theory and including compressibility effects. The analysis was based on linearized equations and used the acceleration potential approach, reference 2.

In the present study, the concept of the acceleration potential was used as a basis for determining the noise due to vibration and blade loading. Since it has been shown by Farassat, reference 3, that blade thickness may be a contributing factor in noise production, thickness noise for a symmetrical airfoil section was included, the analysis of which was based on the velocity potential approach.

The analysis was done for one blade, two or more blades could be treated by a proper phasing of the one bladed results. The calculated results are given in terms of pressure time histories at an observation point that moves at the forward velocity of the propeller. The analysis applies to both near and far field problems since no distance approximations were made.

Symbols

a	speed of sound
A	area
b	half chord
$c(x)$	chord function
C_{L_α}	lift coefficient
$F(\tau)$	doublet strength
h	bending displacement function
h_o	bending displacement magnitude
M_t	tip Mach no.
n_o	normal to velocity vector at x_o, θ_o, r_o
$P(t)$	total pressure = $P_L + P_T$
P_T	thickness pressure
P_L	lift pressure
r_o	radial distance of pulse to propeller axis
t	time of arrival of pulse at field point (x,y,z)
U	forward velocity
V	total velocity at r_o
x_o	source point location - distance from propeller plane - positive aft
x,y,z	field point location
$\xi(\tau),\eta(\tau),\zeta(\tau)$	location of source or doublet
τ	time of doublet or source pulse
ε_o	$= \mathrm{Tan}^{-1}(U/r_o\Omega)$
θ_o	angular position of propeller, measured from y-axis
θ_A	geometrical angle of blade at r_o, referred to the plane of rotation
ρ	air density
ψ	acceleration potential
ϕ	velocity potential
Ω	rotational speed
ω	blade vibration frequency
α	angle of attack

Analysis

Since the problem to be treated is linear and since we shall be considering specifically the symmetrical thickness case, the noise due to the thickness and that due to lift are uncoupled. Thus the noise due to thickness and the noise due to lift and vibration can be combined by superposition. First the noise due to lift and vibration shall be treated, then the thickness effect studied.

Derivation of Lifting and Vibration Noise

The concept of the acceleration potential will be used in determining the noise due to lift and vibration. This method was utilized in reference 1 where a lifting surface procedure was developed to determine the surface forces on a propeller in compressible flow. The pressure due to a source or doublet is

*Associate Research Professor of Engineering.
Associate Fellow AIAA
Research funded under NASA Contract NAS1-14605-13

$$p = \rho\psi \tag{1}$$

where ψ is the acceleration potential and ρ is the air density. The expression ψ for a source that is rotating with angular velocity Ω and translating at a uniform velocity U in the negative x-direction is given in reference 1. In reference 1, interest was centered on determining the forces on the blade, consequently, the field point rotated and translated with the same values as the source point. In the present case, we are interested in the case of a field point that is not rotating but is translating at the same velocity and direction as the source point. Thus the expression for ψ is slightly different from that presented in reference 1. The coordinate system is shown in figure 1. The angular position of the disturbance (source or doublet) is given by $\theta_o = \Omega\tau$, the radial distance from the propeller axis to the source point is denoted by r_o. The field (or observation) point is given by x,y,z which are moving at a velocity U in the negative x-direction.

The acceleration potential Ψ of a source may be written as

$$\Psi = \frac{1}{4\pi}\frac{F(\tau)}{D} \tag{2}$$

where

$$D = s + \frac{1}{a}\{(x-x_o)U-(t-\tau)U^2 + y\, r_o\Omega\sin\theta_o - z r_o\Omega\cos\theta_o\}$$

and

$$s = \{((x-x_o)-(t-\tau)U)^2 + (y-r_o\cos\theta_o(\tau))^2 + (z-r_o\sin\theta_o(\tau))^2\}^{1/2}$$

An auxilary equation is given below which relates the time "τ" when a pulse (located at r_o, θ_o, x_o) to the time "t" when the signal reaches the field point (located at x,y,z).

$$(a^2-U^2)(t-\tau) = -(x-x_o)U + (a^2(x-x_o)^2+(a^2-U^2)(y^2+z^2+r_o^2-2r_o(y\cos\theta_o(\tau)+z\sin\theta_o(\tau))))^{\frac{1}{2}} \tag{3}$$

In order to create a pressure discontinuity across the airfoil, a doublet is needed and the expression for a doublet may be obtained by taking a derivative of a source in a direction normal to the velocity vector at r_o, θ_o, x_o.

For this case, the normal derivative is

$$\frac{\partial}{\partial n_o} = -\cos\varepsilon_o\frac{\partial}{\partial x_o} - \frac{\sin\varepsilon_o}{r_o}\frac{\partial}{\partial\theta_o} \tag{4}$$

where n_o is the normal to the velocity vector at x_o, θ_o, r_o

Applying this expression to Ψ results in

$$\Psi D = \frac{\partial\Psi}{\partial n_o} = -\frac{D\frac{\partial F(\tau)}{\partial n_o} - F(\tau)\frac{\partial D}{\partial n_o}}{4\pi D^2} \tag{5}$$

$F(\tau)$ represents the pressure difference across the lifting surface at the location of the doublet. At this point in the analysis, $F(\tau)$ is not known. As a matter of fact it represents the unknown pressure when one is interested in solving for the pressures on a propeller by satisfying certain boundary conditions such as was done in reference 1. Of course, experimentally derived pressures could be inserted if they are known. For the present case, a two dimensional pressure distribution was used for simplicity to determine $F(\tau)$. Utilizing the two-dimensional lift distribution across the chord c(x), the following form is used

$$\sqrt{\frac{b-c(x)}{b+c(x)}}$$

This expression provides the shape of the pressure distribution but does not give the magnitude in pressure units. In order to determine this multiplying factor, the lift on an airfoil in its standard form is equated to the integral of the distribution multiplied by an unknown quantity B. Since the lift distribution can be integrated in closed form, B can be calculated, and thus $F(\tau)$ determined as follows

$$\frac{1}{2}\rho v^2 C_{L_\alpha}\alpha\, A = Bb\int_{-1}^{+1}((1-c(x)/b)/(1+c(x)/b))^{\frac{1}{2}}\, d(c(x)/b)$$

Integrating and solving for B results in the pressure

$$F(\tau) = 2\frac{\rho v^2}{2} C_{L_\alpha}\frac{\alpha A}{b\pi}((1-x_o/\cos\varepsilon_o)/(1+x_o/\cos\varepsilon_o))^{\frac{1}{2}}$$

The instantanious angle of attack α may be written as

$$\alpha = \theta_A - \varepsilon_o - \frac{\dot{h}}{V} - \frac{\dot{\gamma}\, x_o}{V\cos\varepsilon_o}$$

where γ is the angle of a torsion vibration mode and $\dot{\gamma}\, x_o/V\cos\varepsilon_o$ represents an equivalent angle; θ_A is the geometric angle of the blade at r_o measured from the plane of rotation; h is the displacement of the blade in a bending vibration mode and h/V represents an equivalent angle of attack at,

r_o, x_o; $V^2+r_o^2\Omega^2+U^2$; and $\varepsilon_o = \tan^{-1}\frac{U}{r_o\Omega}$

Assuming the vibration modes are harmonic

$$h = h_o\cos\omega_h\tau$$

$$\gamma = \gamma\ \cos\omega_\gamma\tau$$

where ω_h is the bending frequency, ω_γ is the torsional frequency and h_o and γ_o represents the deflection mode shapes as functions of r_o. then

$$\alpha = \theta_A - \varepsilon_o + \frac{h_o \omega_h \sin \omega_h \tau}{V} + \frac{\gamma_o x_o \omega_\gamma \sin \omega_\gamma \tau}{V \cos \varepsilon_o} \quad (7)$$

Returning to the expression for the doublet, Eq. 5, and applying equation 4, there is obtained

$$\psi_D = \frac{1}{4\pi D^2} \{D(-\cos \varepsilon_o \frac{\partial F(\tau)}{\partial x_o} - \frac{\sin \varepsilon_o}{r_o} \frac{\partial F(\tau)}{\partial \theta_o}) + F(\tau) (\cos \varepsilon_o \frac{\partial D}{\partial x_o} + \frac{\sin \varepsilon_o}{r_o} \frac{\partial D}{\partial \theta_o})\} \quad (8)$$

Examining the derivative of $F(\tau)$,

$$\frac{\partial F(\tau)}{x_o} = \frac{\partial F(\tau)}{\partial \tau} \quad (\frac{\partial \tau}{\partial x_o}) \; ; \; \frac{\partial F(\tau)}{\partial \theta_o} \quad (\frac{\partial \tau}{\partial \theta_o})$$

$$\frac{\partial F(\tau)}{\partial \tau} = 2(\rho \frac{V^2}{2}) \frac{C_{L_\alpha}}{b\pi} A \left(\frac{1-x_o/\cos \varepsilon_o}{1+x_o/\cos \varepsilon_o}\right)^{\frac{1}{2}} (\frac{h_o \omega_o^2 \cos \omega_h \tau}{V} + \frac{\gamma_o \omega_\gamma^2 \cos \omega_\gamma z}{V \cos \varepsilon_o})$$

The quantities $\frac{\partial \tau}{\partial x_o}$, $\frac{\partial \tau}{\partial \theta}$ can be determined from Eq. (3).

$$\frac{\partial z}{\partial x_o} = \frac{(x-x_o) - (t-\tau)\, U}{aD} \text{ and}$$

$$\frac{\partial \tau}{\partial \theta_o} = \frac{-y_o r_o \sin (\Omega\tau) + z r_o \cos (\Omega\tau)}{as + (x-x_o)U - (t-\tau)U^2}$$

The remaining terms to be determined $\frac{\partial D}{\partial x_o}$, $\frac{\partial D}{\partial \theta_o}$, are given below. The quantity D is defined following equation (2).

$$\frac{\partial D}{\partial x_o} = \frac{\partial s}{\partial x_o} + \frac{1}{a} \{- U + \frac{\partial \tau}{\partial x_o} U^2 + y r_o \Omega^2 \cos (\Omega\tau) \frac{\partial \tau}{\partial x_o} + z_o r_o \Omega^2 \sin (\Omega\tau) \frac{\partial \tau}{\partial x_o}\}$$

where

$$\frac{\partial s}{\partial x_o} = \frac{1}{s} \{(x-x_o) - (t-\tau)U)(U \frac{\partial \tau}{\partial x_o} - 1) + y r_o \Omega \sin \Omega\tau \frac{\partial \tau}{\partial x_o} - z r_o \Omega \cos \Omega\tau \frac{\partial \tau}{\partial x_o}\}$$

$$\frac{\partial D}{\partial \theta_o} = \frac{\partial s}{\partial \theta_o} + \frac{1}{a} \{U^2 \frac{\partial \tau}{\partial \theta_o} + y r_o \Omega \cos \Omega\tau + z r_o \Omega \sin \Omega\tau\}$$

$$\frac{\partial s}{\partial \theta_o} = \frac{1}{s} \{(x-x_o)-(t-\tau)U)U \frac{\partial \tau}{\partial \theta_o} + y r_o \sin \Omega\tau - z r_o \cos \Omega\tau\}$$

This completes the derivation of the pressure $P_L = \rho\psi$ at a point x,y,z due a doublet located at r_o, $\frac{x_o}{\cos \varepsilon_o}$, θ_o. The next section is concerned with a derivation of the noise due to thickness.

Noise Due to Thickness

Bernoullis' equation may be written as

$$P_T = \rho(\frac{\partial \phi}{\partial t} + U \frac{\partial \phi}{\partial x}) \quad (10)$$

where ϕ is the velocity potential. The expression for the velocity potential ϕ is identical to that used for the acceleration potential with the exception that $F(\tau)$ is replaced by a value that is constant with regard to time since a time variation of the source would simulate a pulsating body.

Therefore

$$\phi = \frac{F}{4\pi D} \quad (11)$$

The strength of the source F is directly related to the velocity normal to the surface or

F = Slope x Stream velocity (for small slopes)

or

F = (SL) (V)

where

$V = (r_o^2 \Omega^2 + U^2)^{1/2}$

SL = slope of airfoil surface at location of source

$$\frac{\partial \phi}{\partial t} = -\frac{1}{4\pi} \frac{(SL)(V)}{D^2} \{\frac{\partial s}{\partial t} + \frac{1}{a} ((\frac{\partial \tau}{\partial t} - 1)U^2 + y r_o \Omega^2 \cos \Omega\tau \frac{\partial \tau}{\partial t} + z r_o \Omega^2 \sin \Omega\tau \frac{\partial \tau}{\partial t})\}$$

$$\frac{\partial s}{\partial t} = \frac{1}{s} \{(x-x_o)-(t-\tau)U)\; U(\frac{\partial \tau}{\partial t} - 1) + y r_o \Omega \sin \Omega\tau \frac{\partial \tau}{\partial t} - z r_o \Omega \cos \Omega\tau \frac{\partial \tau}{\partial t}\}$$

where $\frac{\partial \tau}{\partial t} = \frac{sl}{sl + r_o y \Omega \sin \Omega\tau - r_o z \Omega \cos \Omega\tau}$

$$sl = \{a^2(x-x_o)^2 + (a^2-U^2)(y^2 + z^2 + r_o^2) - 2r_o(y \cos (\Omega\tau) + z \sin (\Omega\tau))\}^{1/2}$$

For the derivative with respect to x.

$$\phi = \frac{1}{4\pi} \frac{(SL)V}{D}$$

$$\frac{\partial \phi}{\partial x} = - \frac{(SL)(V)}{4\pi D^2} \frac{\partial D}{\partial x}$$

$$\frac{\partial D}{\partial x} = \frac{\partial s}{\partial x} + \frac{1}{a} \{U - \frac{\partial t}{\partial x} U^2\}$$

$$\frac{\partial s}{\partial x} = \frac{1}{s} \{(x-x_o) - (t-\tau)U)(1- \frac{\partial t}{\partial x} U)\}$$

$$\frac{\partial t}{\partial x} = \frac{1}{a^2-U^2} \{-U + \frac{a^2(x-x_o)}{sl}\}$$

This completes the derivation of the thickness effects.

Computational Procedure

The pressure at a field point x,y,z will be the integral of the sum of equations 1 and 10,

$$P(t) = \int_A (P_L + P_T)\, dA$$

over the area of the propeller blade at a given time t. The integration was accomplished by using a rectangular distribution in the span and chord directions. Thus the value of the integrand was calculated at a selected point on the blade and multiplied by a differential area Δ A with the selected point in the center of the area.

One complication arose due to the necessity of properly accounting for retarded time. This was handled in the following manner. A time "τ" was chosen, which represents a position of a source point on the blade. Corresponding to the time τ, a position was selected on the blade, which for convenience was the farthest outboard span position and located in the center of the chord (x_o=0). The time of arrival "t" at the field point x,y,z of a pulse created at time "τ" was calculated from equation (3).

When the disturbance point is moved to another position on the blade, it is necessary that the pulse arrives at time t, in order to sum all the pressure pulses from all points on the blade which arrive at the same time. Therefore, with a new pulse location, it is necessary to insert the time t into equation 8 and solve for τ. With τ calculated, then the pressure pulse from that position on the blade can be calculated and added to the pulses from the other positions on the blade, all of which arrive at the same time t at the field point. When all the source points on the blade have been calculated and added, a new τ is selected and the entire process repeated. For the present calculation, one complete revolution of the propeller was divided into 1000 parts and consequently a time history of the pressure is obtained.

The results of sample calculations are presented in the next section. The propeller was divided into 20 chordwise pulse points and 20 spanwise sections. In order to reduce the computation time, the 5 spanwise stations nearest the hub were eliminated and the results were compared to the results obtained with a complete 20 station results and no appreciable difference was found. Thus the results for 20 x 15 = 300 integration areas were used. Since the calculations were repeated 1000 times, a total of 300,000 points were calculated. The properties of the propeller are given in the Table.

Discussion of Results

In this section the results of calculating the noise due to thickness, lift and vibration are given.

On Figure 2 is given the noise in the propeller plane in Newton per square meter plotted against time t at a field point in the propeller disk plane and 7.28 m from propeller axis. Figure 2(a) presents the noise produced by thickness only. The noise is characterized by distinct positive and negative spikes with the pressure essentially zero for the remainder of the time history. Figure 2(b) presents the noise produced by lift only. For this case it was assumed that the propeller was operating with a constant 6° angle of attack throughout the span ($\theta_A - \varepsilon_o = 6°$). It is seen that a similar spike occurs at the same time, but the magnitude is somewhat lower than the noise due to thickness. In addition, the pressure has a small variation with time as opposed to the thickness noise which is virtually zero away from the spike. The total noise is shown in Figure 2(c), which is the sum of the two previous figures.

In the next figure, the effect of vibration is shown for the same in-plane field point location. On Figure 3(a) the time history of the noise is given for a vibration frequency equal to the rotational speed of the propeller. The vibration mode shape used in the calculation corresponded to that for a uniform beam, where the mass and stiffness properties were constant throughout the length of the propeller. The tip deflection was taken as $\pm$ .051 m ($\pm$ 2 in).

This tip amplitude assumption may be felt to be rather large, however, for the case of flutter it is thought to be within the possible amplitude range. Under normal operating conditions, a much smaller tip amplitude would probably be encountered, and hence, a lower noise level would be found. These uniform beam deflection modes and tip deflections were used for all the vibration cases to be discussed in the remainder of the paper. Returning to Figure 3(a), comparing the time history to Figure 2(c), one can observe two effects. First, the noise is following a general sinusoidal shape when observed over the complete cycle, and secondly, the magnitude of the positive and negative peaks have been slightly reduced, thus indicating a surprising beneficial effect.

For the next case, the vibration frequency was increased to twice the rotational speed, Figure 3 (b). Again, the overall vibration pattern can be seen, but the peak amplitudes have been more drastically changed. The positive peak has been significantly reduced by the vibration, but the negative peak has been greatly increased.

It should be realized that the phasing of the vibration mode relative to the rotational position is a variable and changes in this phase relationship will probably change the magnitudes of the peak amplitudes.

For the final frequency, results for a vibration frequency that is 4 times the rotational speed are given in Figure 3(c). The overall time history again shows the sinusoidal noise pattern, but the peaks have again been drastically altered. The positive peak is about 7 times that for the previous case, whereas the negative peak has been just slightly magnified.

For the next case, the field or observation point has been swung on a constant radius to a point ahead of the propeller at an angle of 45°. The time history for the thickness noise is given on Figure 4(a). The positive and negative peaks have both been drastically reduced and, also, the peaks are substantially rounded, both effects would probably reduce the perceived noise due to the reduction in higher harmonic noise components. The thickness noise is given in Figure 4(b). Although the positive peak has increased, the peaks are well rounded and it is estimated that the perceived noise would also be reduced relative to the in-plane case. The final figure of this group contains the total noise, including the vibration noise and is given in Figure 4(c). The positive noise peak is approximately 3 times that shown on Figure 3(c), but again the peaks are broader and more rounded.

The final case to be treated involves moving the observation point forward to the axis of the propeller or 90° from the plane of the propeller. Calculations indicated that no noise would be generated by either the airfoil thickness or steady lifting effects. On the other hand, the noise due to vibration, Figure 5 showed a constant amplitude, sinusoidal noise. Therefore, measurements of noise on the propeller axis should indicate whether a propeller is vibrating or responding dynamically to some disturbing input such as turbulance or random loading.

Additional Calculations

Other calculations have been made but were not included due to space limitation. For instance, a torsion vibration mode shape was used for one case and it was found, at least for that case, that the in-plane noise level was so low compared to the bending vibration noise that noise due to torsional motion could be neglected.

A second bending mode was also run, and the results indicated that the noise level was somewhat below that of the first bending mode.

Concluding Remarks

A calculation procedure has been developed to determine the noise from a vibrating propeller. Included also is the effect of steady loading and airfoil thickness for a symmetrical airfoil section.

For the particular case studied, the in-plane noise is dominated by thickness noise, with lift and vibratory noise secondary.

However, when the observation point is rotated 45° on a constant radius to a point ahead of the propeller plane, steady loading and vibration noise dominates and the thickness noise is negligible.

For the case of the observation point being rotated to 90°, i.e., on the propeller axis, both the thickness and steady loading noise are zero, and a constant amplitude, sinusoidal noise results. Thus, measurements made on the propeller rotation axis should indicate noise due only to vibration or dynamic response modes.

References

1. Runyan, Harry L.: Unsteady Lifting Surface Theory Applied to a Propeller and Helicopter Rotor, Ph.D. Thesis, Loughborough University of Technology, England, July, 1973.

2. Dowell, E.H., Curtiss, Jr., H.C., Scanla, R.H., Sisto, F.: A Modern Course in Aeroelasticity, Sijthoff and Noordhoff, The Netherlands, 1978.

3. Farassat, F., Brown, T.J.: A New Capability For Predicting Helicopter Rotor and Propeller Noise Including the Effect of Forward Motion, NASA TMX-74037, June, 1977.

Table 1 - Blade Characteristics

Radius	= 1.30 m
rpm	= 2145
Chord	= .156 m
Thickness	= $T(r_o) = 0.069 + 3.2244\, e^{-8.05\, r_o}$
Airfoil Shape	= $(C)\ (T(r_o))(3.333E - 6.5079E^2 + 3.1746E^3)$
E	= $(\frac{x_o}{c} - \frac{1}{2})$
Aircraft Speed	= 144.5 km/h
Field Point (In disk plane)	= 7.28 m from propeller hub, moving with aircraft
M_t	= .87
C_{L_α}	= 2π

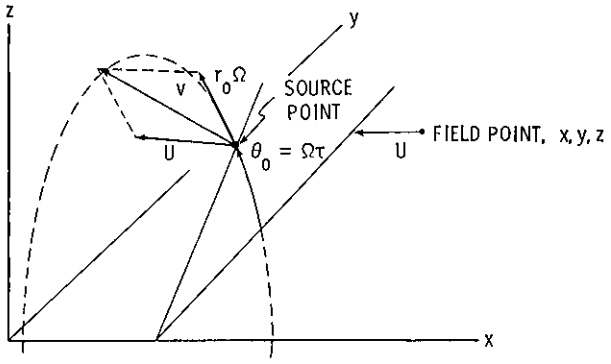

Figure 1(a) Coordinate System

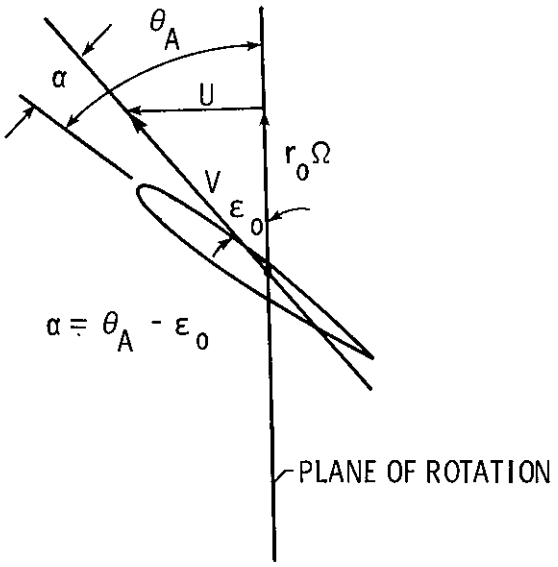

Figure 1(b) Coordinate System - blade cross-section

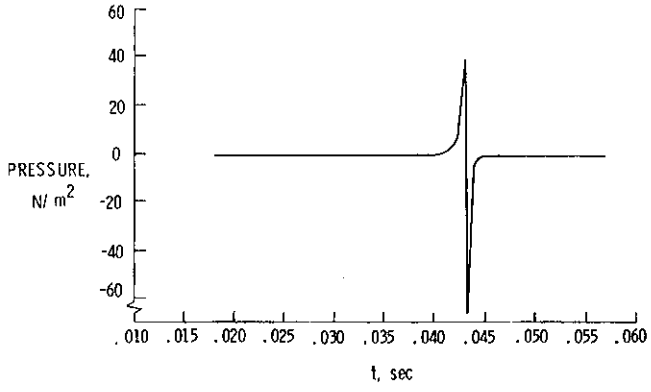

Figure 2(a) Thickness Noise, In-plane

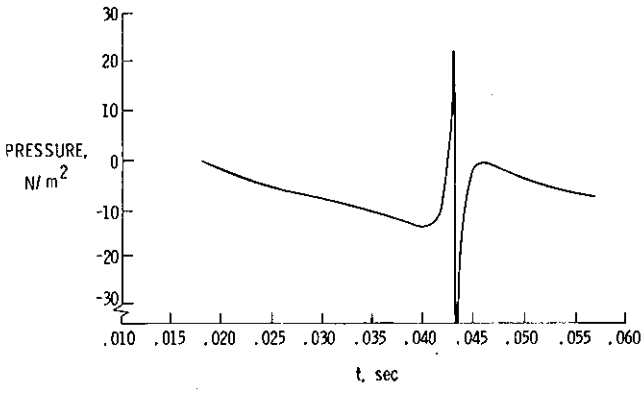

Figure 2(b) Lift Noise, 6° Angle of Attack, In-plane

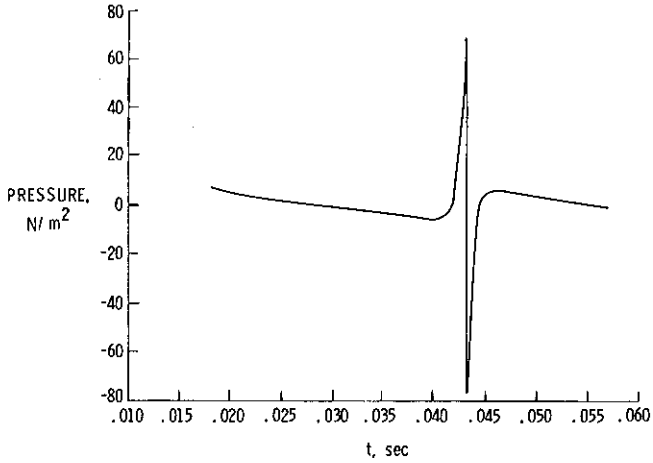

Figure 2(c) Total Noise, 6° Angle of Attack, In-plane

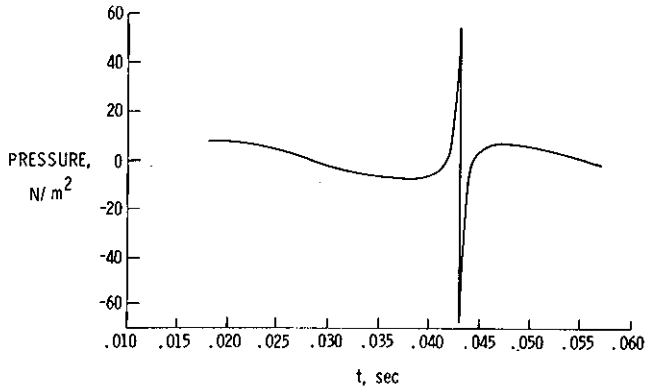

Figure 3(a) Total Noise, In-plane, $\omega_h = \Omega$

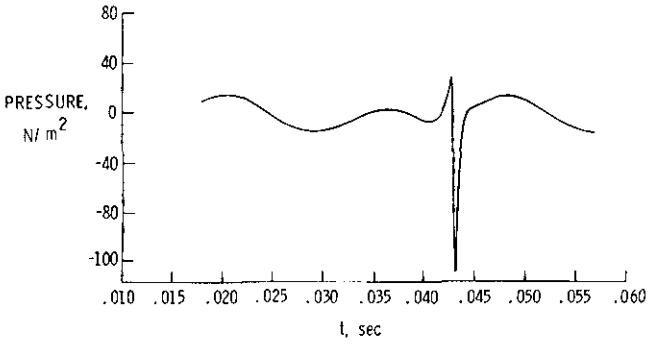

Figure 3(b) Total Noise, In-plane, $\omega_h = 2\Omega$

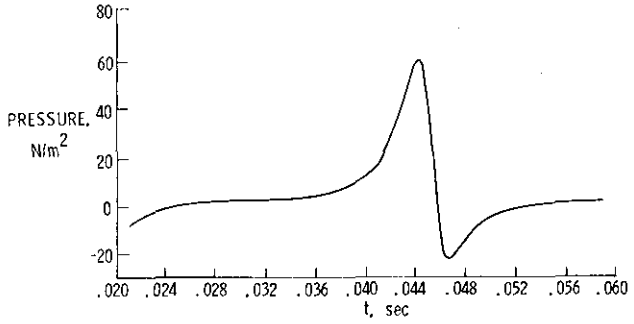

Figure 4(b) Lift Noise, 45° Azimuth

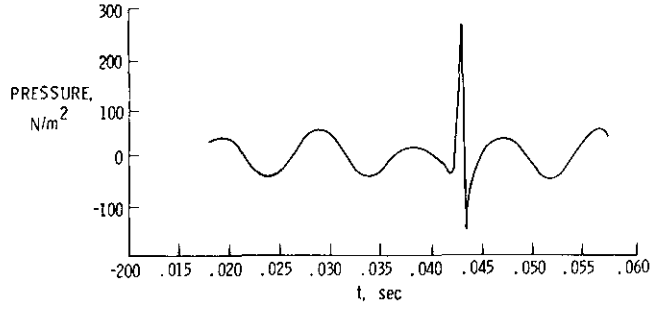

Figure 3(c) Total Noise, In-plane, $\omega_h = 4\Omega$

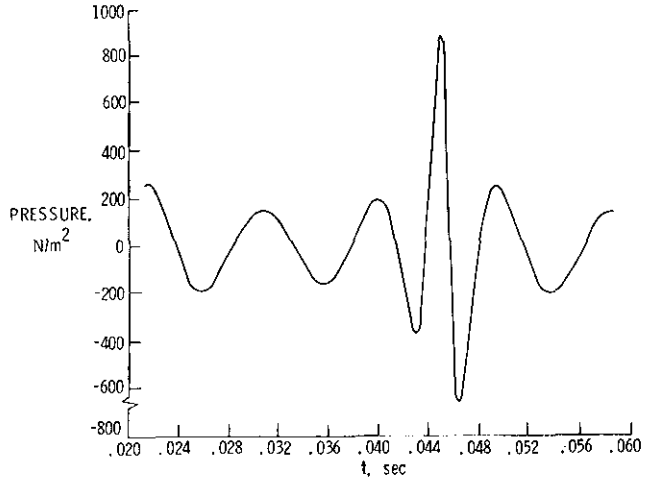

Figure 4(c) Total Noise, 45° Azimuth, $\omega_h = 4\Omega$

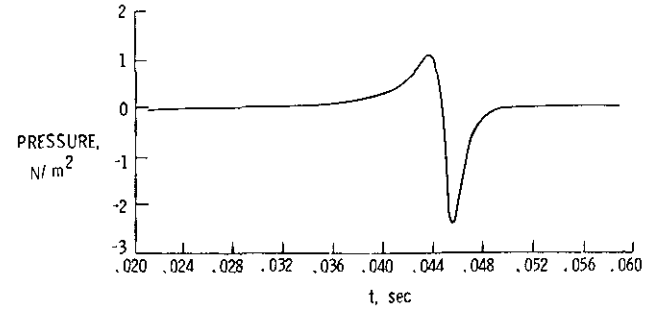

Figure 4(a) Thickness Noise, 45° Azimuth

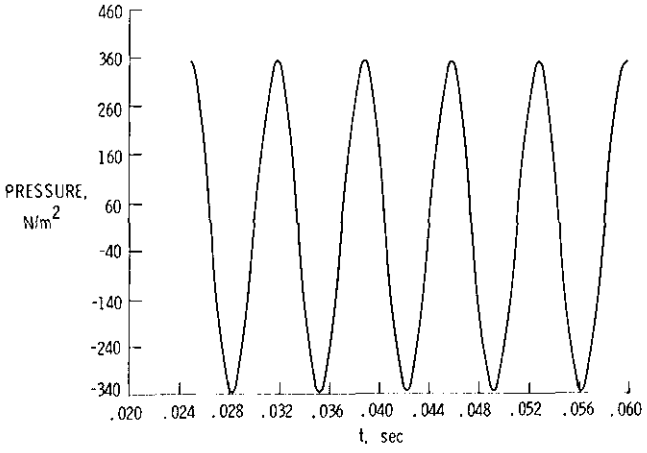

Figure 5 Total Noise, On Propeller Axis, $\omega_h = 4\Omega$